

# REVIEW OF BEAM DYNAMICS AND SPACE CHARGE RESONANCES IN HIGH INTENSITY LINACS

I. Hofmann\*, G. Franchetti, GSI, Darmstadt, Germany

J. Qiang, R. Ryne, LBL, CA 94720, USA

F. Gerigk, RAL, GB, D. Jeon, ORNL, USA and N. Pichoff, CEA, France

## Abstract

Recent systematic studies of resonant space charge effects and anisotropy have helped to narrow the gap between idealized beam physics models of halos and high-current linac design. We review the beam dynamics basis of non-equipartitioned beams, discuss the consequences of bunch anisotropy, and introduce “3D free energy equivalence” as a new concept to model halo growth in linac bunches. Results are applied to the CERN-SPL, the SNS and the ESS superconducting (sc) linac designs.

## 1 INTRODUCTION

Multi-particle simulations for the high power linac designs currently under study predict that rms emittance growth and loss from the outer halo can be sufficiently controlled to meet the requirements specified for Megawatt facilities, e.g. beam loss not exceeding the level of 1 W/m. Since critical theoretical and simulation predictions have so far not been tested by experiments it remains important to develop a systematic picture of the beam physics basis predicting beam quality degradation and losses. This is attempted in the present study by showing that the gap between simple models and complex linacs can be bridged by using three basic concepts: (a) the beam evolution is controlled by *space charge driven resonances* – in spite of the relatively short length of the linacs – involving core-core (related to the issue of equipartition) as well as core-single particle resonances (related to halo); (b) *anisotropy effects* in ellipsoidal bunches to go beyond the simplified halo models developed so far primarily for cylindrical beams (reviewed by Wangler [1]) or spherical bunches; (c) a revival of the concept of *free energy*, originally proposed by Reiser for 1D [2], which we show to be extendable, in a modified sense, to the problem of 3D (details of these concepts are also found in Refs. [3, 4, 5]).

The simulation basis of our comparison relies on the following:

(1) for our extended parameter studies: the IMPACT code [6] with its 3D Poisson solver has the option to run a “3D constant focusing channel” with linear RF force and no acceleration; we use  $10^6$  simulation particles on a  $64 \times 64 \times 64$  grid.

(2) the “CERN-SPL” design, a sc proton linac with final energy of 2.2 GeV studied as driver for a neutrino factory, where only the sc part from 120 MeV to 2.2 GeV (current of 40 mA, corresponding to twice the design current)

is considered in our study [7]; this design is using the IMPACT code as well ( $10^6$  particles and  $64 \times 64 \times 64$  grid).

(3) the “SNS linac” (Spallation Neutron Source), which is designed for 2 MW of 1 GeV  $H^-$ , with a DTL from 2.5 to 85 MeV and a CCL up to 180 MeV followed by the sc SRF [8]; simulations carried out with 3D PARMILA with  $10^5$  particles and using 38 mA current.

(4) the “ESS linac” (European Spallation Source) for 5 MW (114 mA) and 1.3 GeV, with a DTL from 5 to 100 MeV, a CCL up to 250 MeV followed by the sc structure [9]; simulations are carried out with the Saclay code PARTRAN using the PICNIC [10] 3D space-charge routine with  $10^4$  particles.

## 2 STABILITY CHARTS AND “EQUIPARTITIONING”

We first discuss the issue of emittance exchange or growth in non-equipartitioned but rms matched beams. The relevant parameter, the longitudinal to transverse energy ratio, is given by  $T \equiv (\epsilon_z k_z) / (\epsilon_x k_x)$ , hence equipartition implies  $T = 1$ . Note that here and in the remainder of this paper emittances are understood as normalized. It has been shown in the analytical “coherent resonance model” elaborated in Refs. [11, 3, 12] that equipartition is not necessary for bunch stability and emittance conservation. Energy/emittance exchange requires resonant coupling, which can take place only if an intrinsic resonance relationship is fulfilled, where the nomenclature “ $l:m$  resonance” describes an internal difference resonance condition [13].

For practical purposes it is convenient to plug the analytical results for given (initial) emittance ratio into a stability or resonance chart with contour levels for the analytically calculated growth rates shown in the plane of tune depression in one direction (here chosen as  $x$ ) versus the focusing ratio  $k_z/k_x$ . The rates are defined as inverse of the number of betatron periods in  $x$  (without space charge) needed per e-folding of resonant exchange. In Refs. [3, 4] these charts were confirmed by extensive IMPACT 3D simulations in a constant focusing channel. In the following we use these charts calculated for the nominal emittance ratios of the various designs, and plot on them the actual linac tune footprint. This is shown in Fig. 1 for the CERN SPL design [7] and nominal  $\epsilon_z/\epsilon_{x,y} = 2$ . The pronounced 2:2 resonance centered at the tune ratio  $k_z/k_x = 1$  is avoided for the reference design, whereas the modified design (case 2) with increased tune ratio shows overlap with the resonance band mainly at  $k_z/k_x = 1.1$ , where an e-folding distance of only 3 betatron periods is predicted. The distinctive behavior off

\* i.hofmann@gsi.de

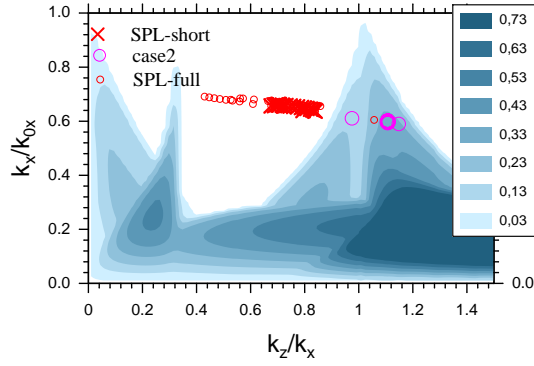


Figure 1: Stability chart for  $\epsilon_z/\epsilon_{x,y} = 2$ : CERN SPL reference and modified (case 2) designs (contour levels: inverse of betatron periods in  $x$  per e-folding of resonance).

and on the stop-band is confirmed by simulations extending over the first two sections of the superconducting linac only, between 120 and 390 MeV (Fig. 2, where the tune footprint of the full sc is also shown). Note that in case 2 the reduction of the longitudinal emittance is more pronounced than the increase of the transverse one, since the “energy” associated with it is shared by *both* transverse degrees of freedom. The exchange is limited to the rms emittance – i.e. a beam core effect – and not accompanied by halo.

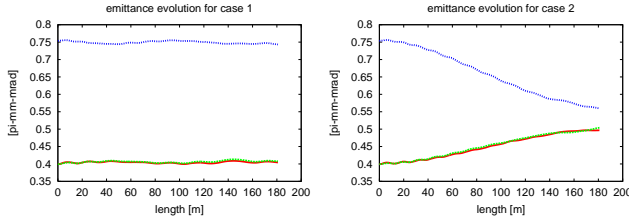


Figure 2: Emittance evolution as a function of distance for nominal design (SPL-short), and for case 2; upper curve in  $z$ , lower curves in  $x, y$ .

A not unexpected feature is that emittance transfer in a resonance band is weakened or vanishes completely, if the beam is nearly or fully equipartitioned there, since there is no free energy available for transfer. This difference is noted in Fig. 3 by inspecting the shrinking of the 2:2 stop-bands with decreasing  $\epsilon_z/\epsilon_{x,y}$ . The chart for  $\epsilon_z/\epsilon_{x,y} = 1.4$  (top) relates to the case of the SNS linac design. Note that in the SNS design the full length corresponds to only 17 betatron periods, defined without space charge. The tune ratio  $k_z/k_x$  varies over a large interval: it intercepts the 2:2 stop-band early in the DTL, drops to 0.3 at the end of it and returns to the 2:2 stop-band in the SRF. The PARMILA simulation shows a small effect of this stop-band (mainly in the DTL): the final transverse (longitudinal) rms emittances change by +27% (+3%), compared with +17% (+20%) for  $\epsilon_z/\epsilon_{x,y} = 1$ , and 40% (-13%) for  $\epsilon_z/\epsilon_{x,y} = 2$ . Note that the growth found in all directions for  $\epsilon_z/\epsilon_{x,y} = 1$  is part

of the non-adiabatic behavior of linacs and due to design constraints, abrupt changes in focusing, etc..

The chart also indicates a 1:2 “third order” resonance at tune ratio 1/2 – absent in Fig. 1 due to equipartition –, and a 1:3 “fourth order” resonance at tune ratio 1/3, which may have a small effect here. The third order resonance can be considered as benign in linacs as it can only grow from initial noise [3] and thus would take much longer a distance than available. Similarly, for the ESS linac (bottom of Fig. 3), with  $\epsilon_z/\epsilon_{x,y} = 1.3$ , an effect of the 2:2 resonance is not expected, which agrees with the simulations. Note that the part of tune footprint overlapping with the stop-band at tune ratio 1/3 is ignorable as it pertains only to acceleration from 5 to 6 MeV. Stop-bands for higher than fourth order modes – not covered by the analytical theory upon which the charts are based – have not been found in the systematic simulations of Ref. [4], hence it can be claimed that the charts described here give a sufficiently complete picture.

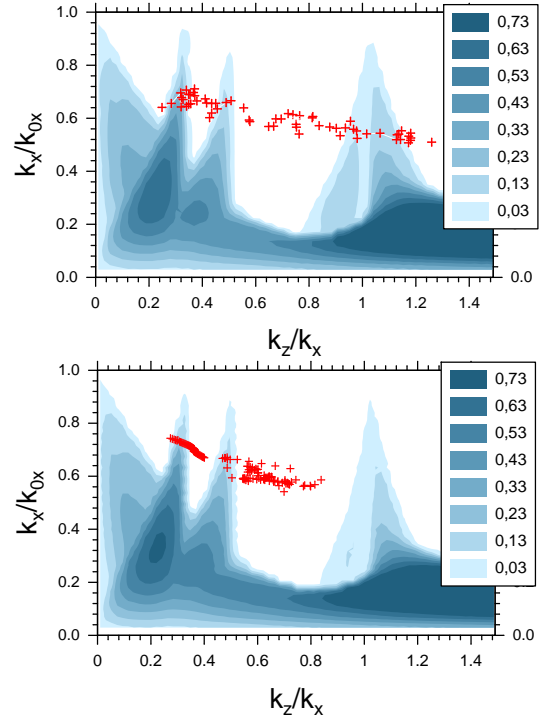


Figure 3: “Tune footprint” of full linac for SNS (top, with  $\epsilon_z/\epsilon_{x,y} = 1.4$ ) and ESS (bottom, with  $\epsilon_z/\epsilon_{x,y} = 1.3$ ).

We conclude by observing that rms emittance conservation of matched beams can be considered as “safe” as long as the major fourth order 2:2 resonance is avoided; if this is not the case,  $\epsilon_z/\epsilon_{x,y}$  should not exceed unity by much.

### 3 MISMATCH AND “FREE ENERGY”

Most of the halo studies in the literature have considered round beams with axi-symmetric focusing, whereas linac bunched beams are known to be anisotropic. Some new aspects caused by anisotropy – with the ratio of tunes and/or emittances as additional free parameters – were dis-

cussed for 2D [14] and 3D beams [15, 16] demonstrating an influence of the mismatch modes on halo size. A systematic study has recently been presented in Ref. [5] for the analogous issue in 2D beams, with the conclusion that anisotropy adds a number of new features to the discussion of mismatch induced halo, which we generalize here to the 3D case. The key to interpreting anisotropic halo growth due to the 2:1 parametric resonance is the dependence on  $k_z/k_x$  of the distance of the fixed-points from the core. These fixed-points are defined as amplitudes, where the mismatch frequency is twice the betatron frequency. According to Ref. [5] the fixed points and outer halo radius for the  $z$ -plane motion move closer to the core, if  $k_z > k_x$  (and similar for  $x$ , if  $k_x > k_z$ ). This counter-intuitive finding of enhanced rms emittance growth in the direction of stronger focusing is explained by the “attraction” of fixed-points, which allows easier population of the halo in the respective plane. As a result the beam becomes more anisotropic and may move away from equipartition.

The quantitative effect of attraction of fixed-points requires self-consistent simulation. A striking conclusion of the preceding 2D study was that the average rms emittance growth,  $(\Delta\epsilon_x/\epsilon_x + \Delta\epsilon_z/\epsilon_z)/2$ , is practically constant over a large range of  $k_z/k_x$  for Gaussian beams, while growth in the individual planes varies with  $k_z/k_x$  according to fixed-point “attraction” [5]. Since  $\Delta\epsilon_x/\epsilon_x + \Delta\epsilon_z/\epsilon_z$  was found largely independent of  $k_z/k_x$ , it could be compared with the “free energy” limit derived earlier by Reiser for  $k_z/k_x = 1$  [2]. The latter is a “1D” approximation understood as the maximum possible rms emittance growth, if all of the energy added to an axially symmetric beam by radial mismatch is “decohered” and a new matched uniform beam is obtained – regardless of the actual driving mechanism. To explore the validity of a *free energy equivalent* average emittance growth in 3D we carried out extensive simulations using the “3D constant focusing channel” option of IMPACT. We chose initially  $\epsilon_z/\epsilon_{x,y} = 1$ ,  $k_x/k_{0x} = 0.6$  and an envelope mismatch by a factor  $M$  equally for all directions as we do in the rest of this study. Such a symmetric mismatch excites a pure “breathing” oscillation for  $k_z/k_x = 1$ , but a mixture of eigenmodes for other tune ratios. Results of the final relative rms emittance growth over 100 periods of betatron oscillation – sufficiently long to get saturation of the phenomena – are shown in Fig. 4 for Gaussian and waterbag (WB) distributions and  $M = 1.3$ . Each run is carried out for a fixed value of  $k_z/k_x$ . The main 2D findings are retrieved in 3D, yet with some alterations:

(a) the averaged rms emittance growth  $(\Delta\epsilon_x/\epsilon_x + \Delta\epsilon_y/\epsilon_y + \Delta\epsilon_z/\epsilon_z)/3$  is found relatively constant for a Gaussian beam and approximated again by the 1D “free energy limit” (see Ref. [5] for the dip near  $k_z/k_x = 1$ , which is explained by an insufficient tail), the growth is significantly less for a WB due to lack of a tail;

(b) growth in the individual planes follows the fixed-point “attraction” principle, which confirms indirectly the dominance of the parametric (2:1) resonance; for the Gaussian it is noted that the longitudinal emittance growth –

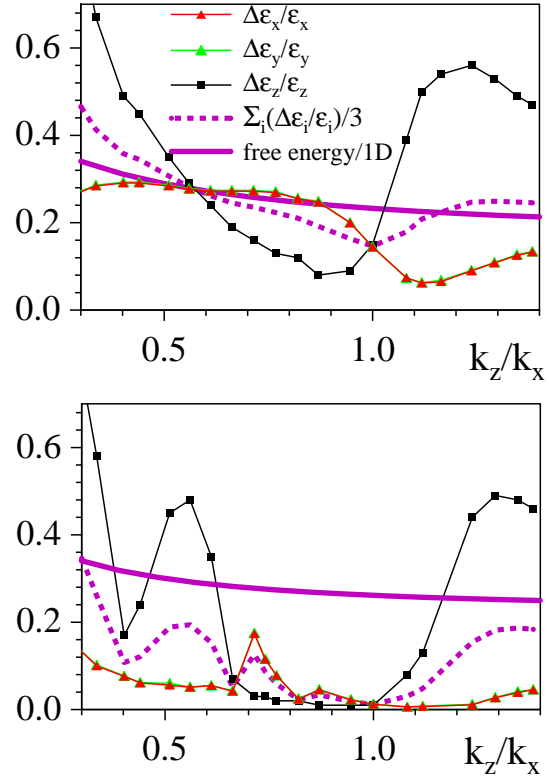


Figure 4: Relative emittance growth from “3D constant focusing channel” simulation for  $M = 1.3$ ,  $\epsilon_z/\epsilon_{x,y} = 1$ ,  $k_x/k_{0x} = 0.6$  and Gaussian (top) and WB (bottom).

dominant for  $k_z/k_x > 1$  – reaches *twice the value of the maximum transverse emittance* growth for  $k_z/k_x < 1$ , which can be understood by observing that the energy added by the mismatch has to “heat” only *one* degree of freedom, if the coupling favors the longitudinal direction;

(c) the “suppression” of the 2:1 resonance for a WB makes the appearance of fourth order resonances more visible, which we expect to drive the peak of the longitudinal emittance near  $k_z/k_x = 0.5$ .

For the “3D free energy equivalence” to become a practically useful tool it is desirable to extend it beyond the specific case of symmetric mismatch in all planes. We propose that an *rms strength for the mismatch* is a proper quantity to describe the average rms emittance growth, hence this could replace the need to distinguish between individual eigenmodes [17]:

$$(M_{rms} - 1)^2 = \frac{1}{3} \sum_{i=x,y,z} (M_i - 1)^2 \quad (1)$$

We point out that the average relative emittance growth can be related to the average entropy growth by using the expressions given by Lawson et al. in 1D [19], e.g.  $S \propto \ln \epsilon$ , which was generalized to 3D by Struckmeier [20]. Hence we have

$$\frac{\Delta S}{k_B} = (\Delta\epsilon_x/\epsilon_x + \Delta\epsilon_y/\epsilon_y + \Delta\epsilon_z/\epsilon_z)/3 \approx \alpha (M_{rms} - 1)^2. \quad (2)$$

Our findings thus connect the average entropy growth with the rms mismatch  $M_{rms}$  using a coefficient  $\alpha$  as in Ref. [5], which depends weakly on tune depression and can be fitted to the results of Ref. [2] – here  $\alpha \approx 2.5$ . The channeling of emittance growth or entropy into  $x, y$  or  $z$ , on the other hand, depends on the type of resonance; in fact, it may be directly opposite to thermodynamics as in the example of Fig. 4, where for  $k_z/k_x > 0.7$  the emittance growth in the originally “hotter” direction is the dominant one.

In Fig. 5 we show the rms emittance growth factors averaged over  $x, y, z$  using initial WB and Gauss distributions for SNS, full sc SPL and ESS, and compare them with the “1D” free energy limit. The growth even for  $M = 1$  is due to the non-ideal behavior of linacs; it is most pronounced (19%) for the SNS simulation, where it apparently covers the mismatch sensitivity up to  $M \approx 1.15$ , and enhances it beyond. Note that for  $\epsilon_z/\epsilon_{x,y} = 1$  the averaged mismatch response is nearly identical. The full linac design of the SNS exceeds the free energy estimate, in spite of the initial WB; the SPL superconducting part, however, stays much below, which is consistent with the “3D constant focusing channel” calculation of Fig. 4 for the WB. A Gaussian input into the SPL superconducting part, on the other hand, leads to a transverse rms emittance growth close to 25%, which agrees well with the prediction of Fig. 4 in the characteristic range of tune ratios for this design, e.g.  $0.4 < k_z/k_x < 0.8$ . This implies that full conversion of the free energy into rms emittance growth (see the corresponding graph in Fig. 5) occurs in the presence of an initial Gaussian tail. In order to explain the contrasting behavior for the WB simulations of the SNS we assume that such tails appear naturally in the low energy linac sections even for initial WB distributions, hence saturated conversion into rms emittance growth can take place in the rest of the linac. A similar conclusion can be drawn for the ESS simulations started at above 20 MeV - avoiding the sensitivity of the WB distribution to the funnel line - which showed growth only slightly exceeding the free energy limit. For the case of the full ESS simulation using realistic RFQ output distribution at 5 MeV, an enhancement of the growth is found for  $M = 1$ , and similar for  $M > 1$ :

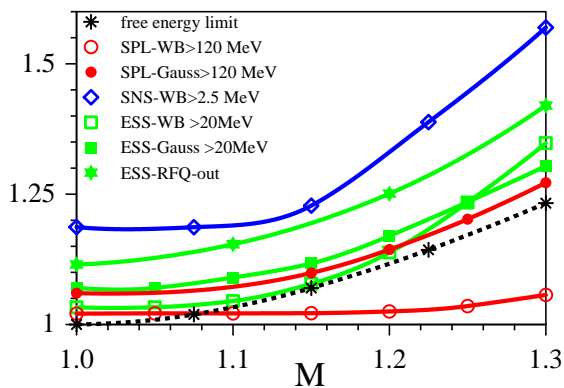


Figure 5: Comparison of averaged rms emittance growth factors vs mismatch.

## 4 ANISOTROPIC HALO SIZE

Halo beyond rms is conveniently quantified by the ratios  $\epsilon_{99\%}/\epsilon_{rms}$  (initially  $\approx 7$  for WB, and  $\approx 9$  for Gaussian) as well as  $\epsilon_{99.99\%}/\epsilon_{rms}$  (initially  $\approx 8$  for WB, and  $\approx 18$  for Gaussian). The relative 99% emittances follow a remarkably similar pattern as the rms emittances, both in their dependence on tune ratio and initial distribution. The Gaussian case (Fig. 6) reflects significant growth by almost a factor 3 in the transverse direction, but visibly less longitudinally. The WB result (not shown) hardly rises above the initial value in the range  $0.6 < k_z/k_x < 1.1$ . Remarkably, the average of 99% emittances over  $x, y, z$  is also quite insensitive to  $k_z/k_x$ , as is the rms. For the 99.99% transverse emittances, instead, the striking feature is that both, Gaussian and WB can reach similarly large values between 50 and 100 in a broad range of  $k_z/k_x$ . We have

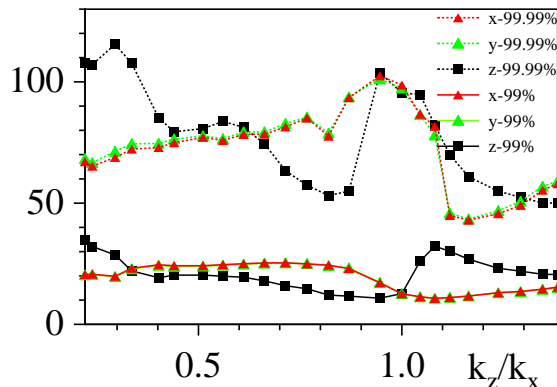


Figure 6: Final 99% and 99.99% emittance relative to final rms emittances for Gaussian case of Fig. 4.

compared these findings with the results from SPL superconducting linac IMPACT simulations shown in Table 1. Noting that the tune footprint of the linac sweeps over the range  $0.4 < k_z/k_x < 0.8$  during acceleration, the agreement on the rms, 99% and 99.99% levels of halo analysis is surprisingly good, even resolved in the individual directions. As discussed in Sec. 3 it must be expected, however, that the suppressed rms and 99% growth of the WB case would disappear if the linac simulation also included the low energy room temperature sections, where the larger number of transitions may enhance initial tail formation.

Table 1: Halo growth factors in  $x/y/z$  for  $M = 1.3$ .

Case	$\epsilon_{rms}/\epsilon_{rms,in}$	$\epsilon_{99}/\epsilon_{rms}$	$\epsilon_{99.99}/\epsilon_{rms}$
SPL WB	1.10/1.05/1.02	7.9/7.5/7.5	76/15/15
SPL Gss	1.43/1.25/1.13	27/21/16	78/73/48

In Fig. 7 we show the 99.99% emittance evolution, which indicates a much more rapidly evolving growth for the Gaussian distribution than for the WB – apparently due to the already existing tails in the initial distribution.

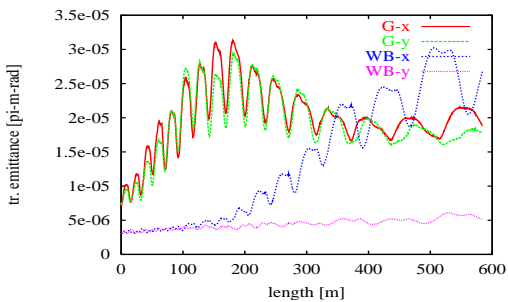


Figure 7: Transverse  $\epsilon_{99.99}$  for  $M=1.3$  and SPL sc linac.

## 5 RANDOM ERRORS

It may be asked to what extent our conclusions apply to the case where mismatch emerges from many small random gradient and RF focusing errors. We have explored this issue in 2D PIC-simulation by using initial Gaussians and a periodic (asymmetric) quadrupole channel with variable  $k_z/k_x$  and given error strength of quadrupole gradients. We found continuous transformation of mismatch into rms emittance growth – linearly with distance along the channel, if averaged over a large number of error sets (see Ref. [21] for details). As for the initial mismatch, the rate of growth averaged over  $z$  and  $x$  is remarkably independent of  $k_z/k_x$ . Hence, it appears that the concept of free energy equivalence is also relevant to the random error case, while the role of the parametric resonance and dependence on initial distributions still need to be explored.

## 6 CONCLUSIONS

Our study has shown that full linac simulations follow the resonance model predictions, inspite of the quite dynamical and complex beam evolution in linacs. Very good agreement was found, in fact, between results for the “3D constant focusing channel” and the SPL sc linac – both using the same code. This comparison allows the following conclusions:

- Sufficiently large *resonance-free regions* exist on the stability charts to make non-equipartitioned design work.
- The parametric 2:1 resonance halo, modified by anisotropy effects, remains the *dominant mechanism to explain halo by initial mismatch*, although higher order halo forming resonances have been identified as well.
- For initial mismatch the rms and 99% emittance growth is significantly enhanced for initially Gaussian distributions as compared with WB; hence sufficient *initial tails* support averaged emittance growth up to the “free energy limit”, while full linac designs moderately exceed this estimate.
- *Collimation of tails* at low energy might be a way to keep growth of rms and 99% emittances noticeably below the free energy limits in the rest of the linac; this is, however questionable for the transverse 99.99% emittance, where Gaussian and WB can lead to similarly large growth up to 50-100 times the rms emittance.

- The “free energy equivalence”, jointly with the rms mismatch strength  $M_{rms}$ , is suggested as useful alternative to the commonly applied multi-parameter eigenmode analysis.

## 7 ACKNOWLEDGMENTS

This work was performed in part using resources of the NERSC scientific computing center of the US DOE.

## 8 REFERENCES

- [1] T.P. Wangler, *Phys. Rev. ST-AB* **1**, 084201 (2000).
- [2] M. Reiser *J. Applied Phys.* **70**, 1919 (1991).
- [3] I. Hofmann, J. Qiang and R. Ryne, *Phys. Rev. Lett.* **86**, 2313 (2001).
- [4] I. Hofmann, G. Franchetti, O. Boine-Frankenheim, J. Qiang, R. Ryne, D. Jeon and J. Wei, in *Proc. of the Particle Accelerator Conference Chicago*, 2001, ed. Y. Cho, p.2902.
- [5] G. Franchetti, I. Hofmann and D. Jeon, *Phys. Rev. Lett.* **88**, 254802 (2002).
- [6] J. Qiang *et al.*, *J. Comp. Phys.* **163**, 434 (2000).
- [7] F. Gerigk *et al.*, in *Proceedings of the Particle Accelerator Conference Chicago*, 2001, ed. Y. Cho, (2001).
- [8] J. Stovall *Proceedings of the Particle Accelerator Conference Chicago*, 2001, ed. Y. Cho, (2001)
- [9] *The ESS project*, Vol III, Technical report, May 2002
- [10] N. Pichoff *et al.*, *Proc. of the Linac Conference Chicago*, 1998, ed. C.E. Eyberger *et al.*, p. 141
- [11] I. Hofmann, *Phys. Rev.* **E 57**, 4713 (1998).
- [12] I. Hofmann and O. Boine-Frankenheim, *Phys. Rev. Lett.* **87**, 034802 (2001).
- [13] A simplified approach would be a single particle resonance condition as used in circular accelerators, e.g.  $lk_z - mk_x = 0$ , which was suggested in Ref. [18]. While this helps to underline the expected order of resonance, it cannot lead to a self-consistent stop-band width.
- [14] M. Ikegami, *Nucl. Instr. and Meth.* **A**, 454, 289 (2000).
- [15] R.L. Gluckstern, A.V. Fedotov, S.S. Kurennoy and R. Ryne *Phys. Rev.* **E 58**, 4977 (1998).
- [16] A.V. Fedotov, R.L. Gluckstern, S.S. Kurennoy and R. Ryne *Phys. Rev. ST Accel. Beams* **2**, 014201 (1999).
- [17] This tentative ansatz is borrowed from a simple harmonic oscillator picture; 2D simulations of Gaussian beams with  $M_{rms} = 1.3$  (equal initial emittances, but different  $k_z/k_x$ ) and broad variation of  $M_x, M_z$  have indeed shown that the resulting rms emittance growth was constant within 10% deviation (unpublished).
- [18] J.-M. Lagniel and S. Nath, *Proceedings of the European Particle Accelerator Conference*, Stockholm, 1998, p. 1118.
- [19] J.D. Lawson, P.M. Lapostolle and R.L. Gluckstern, *Part. Accel.* **5**, 61 (1973).
- [20] J. Struckmeier, *Phys. Rev.* **E 54**, 830 (1996).
- [21] G. Franchetti and I. Hofmann, these Proceedings